AJNR

This information is current as of April 18, 2024.

Functional CT Perfusion Imaging in Predicting the Extent of Cerebral Infarction from a 3-Hour Middle Cerebral Arterial Occlusion in a Primate Stroke Model

Leena M. Hamberg, George J. Hunter, Kenneth I. Maynard, Chris Owen, Pearse P. Morris, Christopher M. Putman, Christopher Ogilvy and R. Gilberto González

Functional CT Perfusion Imaging in Predicting the Extent of Cerebral Infarction from a 3-Hour Middle Cerebral Arterial Occlusion in a Primate Stroke Model

Leena M. Hamberg, George J. Hunter, Kenneth I. Maynard, Chris Owen, Pearse P. Morris, Christopher M. Putman, Christopher Ogilvy, and R. Gilberto González

BACKGROUND AND PURPOSE: Our purpose was to determine whether cerebral perfusion functional CT (fCT), performed after endovascular middle cerebral artery (MCA) occlusion, can be used to predict final cerebral infarction extent in a primate model.

METHODS: fCT with bolus tracking was performed before and 30 and 150 minutes after 3-hour digital subtraction angiography (DSA)–guided endovascular MCA occlusion in five baboons. Parametric cerebral blood flow (CBF), cerebral blood volume (CBV) and mean transit time (MTT) maps were constructed by voxel-by-voxel gamma variate fitting and used to determine lesion sizes. Animals were sacrificed 48 hours after the occlusion, and ex vivo MR imaging was performed. Lesion sizes on fCT and MR images were compared.

RESULTS: Hypoperfusion was clearly identified on all images obtained after MCA occlusion. Thirty and 150 minutes after occlusion onset, respectively, mean lesion sizes were 737 mm^2 ± 33 and 737 mm^2 ± 44 for CBF, 722 mm^2 ± 32 and 730 mm^2 ± 43 for CBV, and 819 mm^2 ± 14 and 847 mm^2 ± 11 for MTT. Mean outcome infarct size on MR images was 733 mm^2 ± 30. Measurements based on CBV and CBF ($R^2 = 0.97$ and $0.96, P < .001$), but not MTT ($R^2 = 0.40, P > .5$), were highly correlated with final lesion size.

CONCLUSION: An endovascular approach to MCA occlusion provides a minimally invasive, reproducible animal model for controlled studies of cerebral ischemia and infarction. Derived cerebral perfusion maps closely predict the 48-hour infarct size after 3-hour MCA occlusion.

To minimize the size of infarction and neurologic disability, new treatment strategies for acute stroke are aimed at rapidly restoring cerebral blood flow (CBF) caused by vascular occlusion. To accomplish this aim, treating physicians need a measure of ongoing ischemia in the early minutes of an occlusion to estimate the extent of irreversible injury and to identify potentially salvageable brain as the target of thrombolytic therapy. Thus, early information about re-

gional cerebral perfusion is necessary to appropriately select different therapies and to determine the prognosis. If repeatable and reproducible, such a technique could also be used to follow up on the patient's progress and to evaluate his or her response to therapy.

Cerebral ischemia occurs when blood flow is reduced to a level that no longer supports the metabolic demands of tissue (1). The early diagnosis of ischemia is more appropriately based on altered cerebrovascular physiology than on secondary morphologic phenomena such as sulcal effacement, loss of gray matter–white matter differentiation, and low attenuation due to edema. If the potential outcome infarct size could be predicted by noting the extent and/or location of early hypoperfusion, patient triage for thrombolytic or neuroprotective therapies could be based on physiologic factors. This goal is attractive because the anatomic changes that are currently used to determine irreversible tissue injury become apparent only later in the evolution of cerebral ischemia and infarction, whereas changes in perfusion are immediately visible if appropriately imaged. Furthermore, physiologic assessment of the amount of ischemic yet

potentially salvageable brain potentially allows rational triage to interventional thrombolytic therapy.

In the current investigation, our aims were twofold: first, to implement a minimally invasive primate occlusion-reperfusion model for studies of stroke and, second, to determine whether the extent of early perfusion deficit, as determined by using functional computed tomography (fCT), can be used to predict the outcome infarction size 48 hours later.

Methods

Animal Model

Animal studies were conducted under the guidelines of our hospital subcommittee on research animal care. Five adult baboons were anesthetized with an intramuscular injection of ketamine (15 mg/kg) mixed with atropine. Anesthesia was maintained by means of mechanical ventilation with 1–2% halothane. The head of each animal was immobilized in a stereotactic frame to achieve more accurate positioning between the control study and the studies performed after occlusion and reperfusion. Use of the same stereotactic frame also ensured consistency in the positioning of different animals. Surgical cutdown was performed to gain vascular access to the femoral artery and vein. A 5F pigtail catheter was placed under fluoroscopic guidance in the inferior vena cava (IVC), and a 7F guiding catheter was maneuvered into a common carotid artery. The IVC catheter was used to administer the iodinated contrast agent for the fCT studies. The carotid guiding catheter was used for digital subtraction angiographic (DSA) studies of the cerebral vasculature and to facilitate placement of an endovascular occlusive device. Unilateral endovascular middle cerebral artery (MCA) occlusion was performed by inflating a 17 Latex Gold valve balloon on a Tracker 18 microcatheter (Target Therapeutics, Freemont, CA) (n = 4) or by placing a Guglielmi detachable coil (Target Therapeutics, Freemont, CA) (n = 1) into an MCA (2). Two animals (animals 3 and 5) received an intravenous injection of anti-P-selectin (Boehringer Ingelheim Inc, Ridgebury, CT) 60 minutes prior to MCA occlusion.

MCA occlusion was maintained for a 3-hour period, and all animals received systemic anticoagulation with intravenously administered heparin. This administration started prior to the introduction of the occluding microcatheter and continued with booster doses until the animal was moved to the recovery area. The intent was to prevent thrombus formation in relation to the occluding microcatheter and thus allow full reperfusion of the vascular territory subtended by the occlusion after removal of the microcatheter. During the period of occlusion, the animal's temperature, blood pressure, and oxygen saturation level were monitored and maintained within normal physiologic ranges. The balloon was deflated or the coil was removed to achieve reperfusion, which was confirmed by means of DSA. After reperfusion and after follow-up imaging was completed, the catheters were removed, the femoral blood vessels ligated, and the cutdown sutured and sprayed with an antibacterial agent. The animals were returned to their cages and extubated. They were monitored for signs of recovery from the anesthesia and given food and water ad libitum.

No less than 48 hours after the occlusion, the animals were sacrificed. The brains were removed and suspended in 10% formalin for 7–10 days to allow fixation. The brains were then examined with ex vivo T2-weighted MR imaging to determine the outcome infarct size.

Imaging Studies

All imaging was performed in an interventional radiology suite by using a hybrid CT and angiographic system (3). The components incorporated into this unit are a C-arm for DSA, a digital fluorography unit, a helical slip-ring CT scanner; the same patient table is used with each modality. The imaging steps were performed in the following sequence. Cerebral perfusion fCT was performed before MCA occlusion; this was the control or baseline study. Balloon or coil occlusion of the selected MCA was then achieved under fluoroscopic guidance. The occlusion was verified by using DSA, after which the animal was moved into the CT scanner. fCT studies were performed at 30 and 150 minutes after the occlusion. At 3 hours after the occlusion, a DSA study was performed to confirm the presence of occlusion; afterward, the balloon or coil was removed, again under fluoroscopic guidance.

DSA Imaging

An MCA was endovascularly occluded by using real-time fluoroscopic monitoring with live digital roadmapping. The success of occlusion was verified with DSA by using a diluted (350 mg I/mL), clinically approved nonionic iodinated contrast agent (Omnipaque; Amersham Health, Princeton, NJ) in a conventional fashion. After successful occlusion was achieved and confirmed, the table was moved into the CT scanner for the fCT studies, which were used to monitor the changes in tissue perfusion resulting from ischemia. After 3 hours of occlusion, DSA imaging was repeated to verify the occlusion. Then, the balloon or coil was removed from the MCA under fluoroscopic guidance and reperfusion was confirmed by using DSA.

fCT Perfusion Imaging

fCT imaging was performed on a nutate/rotate whole-body CT scanner according to a previously published imaging protocol (4). In summary, the anesthetized animal was placed supine in the gantry of the scanner, and its position secured with a stereotactic head holder. A conventional nonenhanced axial image stack was obtained through the brain, graphically prescribed from the lateral scout image. The imaging parameters were a 120-kVp x-ray tube voltage, 200-mA tube current, and a high-resolution imaging mode. The 5-mm section thickness and a 24-cm field of view (FOV) with a 512×512 image matrix yielded a 0.47×0.47-mm (0.22-mm^2) nominal in-plane pixel size. From these axial images, a single section location was chosen for subsequent fCT perfusion imaging. Continuous scanning by means of unidirectional rotation of the x-ray tube around the object commenced 2 seconds before the bolus injection of contrast agent into the IVC, and scanning continued during the injection of contrast agent and for a further 35 seconds. The volume of contrast agent injected was calculated on the basis of the weight of the animal (1.5 mL/kg) and administered at a rate of 15 mL/s. The continuous unidirectional rotation of the x-ray tube provides x-ray photon flux data in the detector ring. The reconstruction of an image uses a 360° segment of this continuous raw data that corresponds to one revolution of the x-ray tube, which takes 1 second. However, the starting point for each reconstructed image does not have to be at the same angular point, and thus, images requiring 1 second of acquisition data could be reconstructed at 100-ms intervals by simply restarting the reconstruction process every 36°. This approach results in images that are overlapped in time, which enable a better characterization of the time-enhancement curves for each voxel because a change in average contrast agent concentration over 1 second can be demonstrated at 100-ms intervals (4). All contrast material injections were performed with a conventional angiographic power injector.

MR Imaging

MR imaging was performed ex vivo by using a 1.5-T whole-body magnet. The formalin-fixed brains were placed in the MR

machine in an orientation as close as possible to that used for CT scanning. MR images were acquired with localizer sections, followed by a graphical prescription of the section orientation to correct for differences between the CT and MR images. T2-weighted images were obtained by using a TR/effective TE of 4200/95 with an echo train length of 16. The outcome infarct size was determined from the section that anatomically corresponded to the section that was used for the CT perfusion studies.

Data Analysis

Construction of Functional Maps.—A series of CT scans were acquired during the first circulation of a bolus of contrast agent (Omnipaque 350 mg I/mL) through cerebral tissue. From these images, the change in contrast agent concentration from the baseline value, measured as a change in Hounsfield number (ΔHU), was calculated voxel-by-voxel for each time point. Gamma variate functions were fitted to these curves to remove the effect of recirculation and noise (4, 5). Voxels that did not receive blood flow, and thus contrast agent, did not demonstrate an increase in the Hounsfield unit value. Prior to gamma variate fitting, these no-flow voxels were identified in an automated fashion by comparing the obtained values with the calculated standard deviation of the baseline value in the voxel. If the time-concentration curve for that voxel remained below the threshold limit, no fitting was attempted, and a value of zero was assigned for that voxel on a parametric map. Otherwise, the fitting was performed. Afterward, parametric maps representing the cerebral blood volume (CBV), CBF, and mean transit time (MTT) were constructed.

Changes in Ischemic Area and Perfusion.—At each time point, the ischemic or hypoperfused area was visually identified without reference to the outcome MR image, and its size was measured on the CBV and CBF maps. Similarly, the area with a prolonged transit time was identified on the MTT maps. The outcome infarction size was determined from the area of hyperintensity on the ex vivo T2-weighted MR image of the brain as it appeared at the time of the animal's sacrifice, at least 48 hours after occlusion. To identify corresponding sections on MR and CT images, we used a visual, anatomically based registration paradigm to select matching section locations. In one animal (animal 3), the MR data set required resectioning with commercial software (Dicer; Spyglass Inc, Champaign, IL) prior to the selection of a matching section location. Because a first-pass CT perfusion image could be obtained at only a single section location, the size of the ischemic region was measured as an in-plane surface area (in square millimeters) rather than as a total volume.

Two observers (L.M.H., G.J.H.) independently measured the lesion sizes on each of the fCT and MR images. Each observer performed the measurements four times for each type of map, at each time point, and for each animal. The result was that a total of 216 regions of interest (ROIs) were measured on fCT images, and 40 measured were on MR images. From these data, intra- and interobserver variabilities were calculated. Intraobserver variability was the coefficient of variation of a set of measurements, that is, the standard deviation of the measurements divided by their mean value expressed as a percentage. Interobserver variability was determined by using an analysis of variance (ANOVA). Statistical analysis was performed by using SAS software (SAS Institute Inc, Cary, NC).

Neurobehavioral Evaluation.—The neurologic evaluation used to establish deficits was adopted from the previous work of Jones et al (1). A five-point scale was used, as follows: A score of 0 indicated no clinical deficit; 1, minimal clinical deficit with decreased dexterity of the contralateral hand; 2, mild clinical deficit, posturing of the contralateral arm at rest, difficulty with contralateral leg during climbing, and facial paresis; 3, moderate clinical deficit, pronounced contralateral hemiparesis, facial paresis, ipsilateral circling, and hemianopsia; and 4,

severe clinical deficit, hemiplegia, inability to stand, and marked ipsiversive turning of the eyes and head.

Results

The data for all animals were analyzed. Animal 2 was excluded from the calculations of average values because leakage of the occluding balloon prevented the creation of a stable region of hypoperfusion for the desired 3 hours. In one animal (animal 5), the CT perfusion image obtained 150 minutes after occlusion could not be recovered because of technical issues with the scanner. The CBF, CBV, and MTT values and outcome lesion sizes determined by the two independent observers, for each animal and each time point, are presented in Tables 1 and 2. CBF and CBV lesions in each animal are close to the outcome infarct size. In one animal (animal 4), lesion sizes measured on the MTT maps are clearly larger than the outcome infarct size.

In Figure 1, the lesion size, as measured in each type of physiologic map, is graphically presented for animals 1, 3, 4 and 5. The final outcome size, as measured on T2-weighted MR images, is presented in each graph as a horizontal line to facilitate easy comparison between the outcome infarct size and the fCT lesion sizes at each time point. The sizes of the hypoperfused lesions, as measured by using CBV and CBF, did not change between the 30- and 150-minute time points after occlusion. In animal 5, no data were available at 150 minutes after occlusion. In animal 4, the MTT lesion sizes at both time points were larger than the outcome infarct size. In three other animals (animals 1, 3, and 5) the MTT lesion sizes were similar to the outcome infarct size. Two of the animals (animals 1 and 3) had large outcome infarcts ($873 \text{ mm}^2 \pm 10$ and $880 \text{ mm}^2 \pm 5$), one (animal 5) had an intermediate infarct ($704 \text{ mm}^2 \pm 10$), and one (animal 4) had a small infarct ($475 \text{ mm}^2 \pm 7$).

Figure 2 shows the correlations between the CBF, CBV, and MTT lesion volumes and the outcome infarct sizes. Animal 2 was excluded because of technical issues with balloon leakage during the study. The results obtained at 30 and 150 minutes were statistically compared by using the Student t test, which showed no significant difference in these results ($P < .001$). On the basis of this finding, the size measurements were pooled for each map type for the purpose of regression analysis. Both CBV- and CBF-based lesion sizes were highly correlated with the outcome lesion size ($R^2 = 0.97$, and 0.96, $P < .001$), as depicted on MR images. The lesion sizes, as measured from the MTT maps, were poorly correlated with the outcome infarct size ($R^2 = 0.40$, $P > .05$).

Figure 3 shows the physiologic CBF, CBV and MTT maps for animals 3 and 5 obtained at baseline and 30 minutes after onset of occlusion. In animal 3, after occlusion of the right MCA proximal to the anterior temporal artery, CBF is reduced in the right temporal lobe, parts of the right putamen and globus pallidus, and parts of the right thalamus. In animal 5, after occlusion of the distal M1 segment of the left

TABLE 1: Repeated measurements of lesion sizes

	Observer 1 Measurements (mm^2)							Observer 2 Measurements (mm^2)						
	CT Perfusion							CT Perfusion						
	30 Minutes			150 Minutes				30 Minutes			150 Minutes			
Baboon	CBF	CBV	MTT	CBF	CBV	MTT	MRI	CBF	CBV	MTT	CBF	CBV	MTT	MRI
1	878	888	878	847	845	846	912	864	897	886	897	907	856	882
2	818	815	775	376	329	334	413	840	854	845	384	386	396	382
3	865	829	855	817	929	844	901	888	869	843	903	844	905	873
4	422	399	775	402	405	709	495	453	463	915	493	469	875	484
5	756	731	749	ND	ND	ND	696	704	709	726	ND	ND	ND	724
1	884	885	857	874	857	847	834	840	884	905	894	850	917	865
2	844	833	844	346	317	331	404	868	858	832	403	406	413	370
3	840	811	819	909	871	801	884	877	908	874	904	905	849	879
4	422	398	819	408	396	797	493	493	482	921	462	498	852	472
5	776	671	707	ND	ND	ND	684	715	685	683	ND	ND	ND	732
1	909	881	872	911	896	868	863	865	847	920	849	874	847	858
2	862	868	840	392	350	322	379	826	833	839	382	376	406	383
3	909	868	859	903	892	876	863	881	889	850	862	859	823	890
4	415	403	763	412	401	750	434	464	501	852	488	485	917	488
5	759	712	688	ND	ND	ND	655	710	711	722	ND	ND	ND	736
1	920	893	915	931	832	883	912	909	871	868	867	925	898	863
2	852	850	805	392	379	359	369	871	819	820	401	391	413	377
3	948	855	844	907	874	860	887	861	902	866	849	828	878	861
4	409	406	774	421	401	762	460	478	470	837	479	471	876	472
5	749	711	651	ND	ND	ND	683	729	683	707	ND	ND	ND	725
	Coefficient of Variation (%)*							Coefficient of Variation (%)*						
1	2.2	0.6	2.8	4.2	3.2	2.1	4.4	3.3	2.5	2.5	2.6	3.7	3.8	1.2
2	2.3	2.7	4.0	5.8	7.9	4.7	5.3	2.5	2.1	1.3	2.8	3.2	2.0	1.7
3	5.4	3.0	2.1	5.1	3.0	3.8	1.8	1.3	2.0	1.7	3.2	3.8	4.1	1.4
4	1.5	0.9	3.1	1.9	1.0	4.8	6.2	3.7	3.5	4.9	2.9	2.7	3.1	1.7
5	1.5	3.6	5.8	ND	ND	ND	2.6	1.5	2.2	2.7	ND	ND	ND	0.8

* Average variabilities were 3.7% for observer 1 and 2.1% for observer 2. No statistically significant differences in interobserver or intraobserver variabilities were present, as measured by using ANOVA ($P > 0.36$).

TABLE 2: Hypoperfused and outcome lesion sizes

	Lesion Areas*							
	30 Minutes			150 Minutes			Outcome	Neurobehavior
Baboon	CBF	CBV	MTT	CBF	CBV	MTT	Size†	Score
1	884 ± 10	881 ± 6	888 ± 8	884 ± 11	873 ± 12	870 ± 9	873 ± 10	4
2	848 ± 7	841 ± 7	825 ± 9	384 ± 6	367 ± 11	372 ± 14	385 ± 6	0
3	884 ± 12	866 ± 12	851 ± 6	882 ± 12	875 ± 12	854 ± 12	880 ± 5	3
4	444 ± 11	440 ± 15	832 ± 22	445 ± 14	441 ± 16	817 ± 26	475 ± 7	0
5	737 ± 9	702 ± 7	704 ± 11	No Data	No Data	No Data	704 ± 10	0
Mean ± SEM‡	737 ± 33	722 ± 32	819 ± 14	737 ± 44	730 ± 43	847 ± 11	733 ± 30	

* Hypoperfused lesion sizes (in square millimeters) as measured with perfusion CT at 30 and 150 minutes after the start of occlusion.

† The outcome lesion size is measured with MR imaging at 48 hours.

‡ Data in baboon 2 are not included in the calculation of the mean values.

MCA, the basal ganglia is preserved, with hypoperfusion in the left temporal lobe. In both animals, lesion sizes are similar on all maps.

Figure 4 shows the DSA images in animal 5 that verified the left MCA occlusion and subsequent reperfusion. After reperfusion, flow in the left MCA branches was clearly seen.

Figure 5 shows the pre- and postocclusion fCT maps for animal 4. The right MCA is occluded, with minimal involvement of the distal perforators. This occlusion has resulted in ischemia and infarction, mainly in the right temporal lobe, with subtle reduced perfusion in the right putamen and external capsule. (This involvement is demonstrated by *red* ROIs overlaid on gray-scale images of the CBV, CBF, and MTT maps in the *bottom row*.) However, the apparent lesion is larger on the MTT map than on the CBV and CBF maps. This animal had a substantial collateral blood supply to the distal right
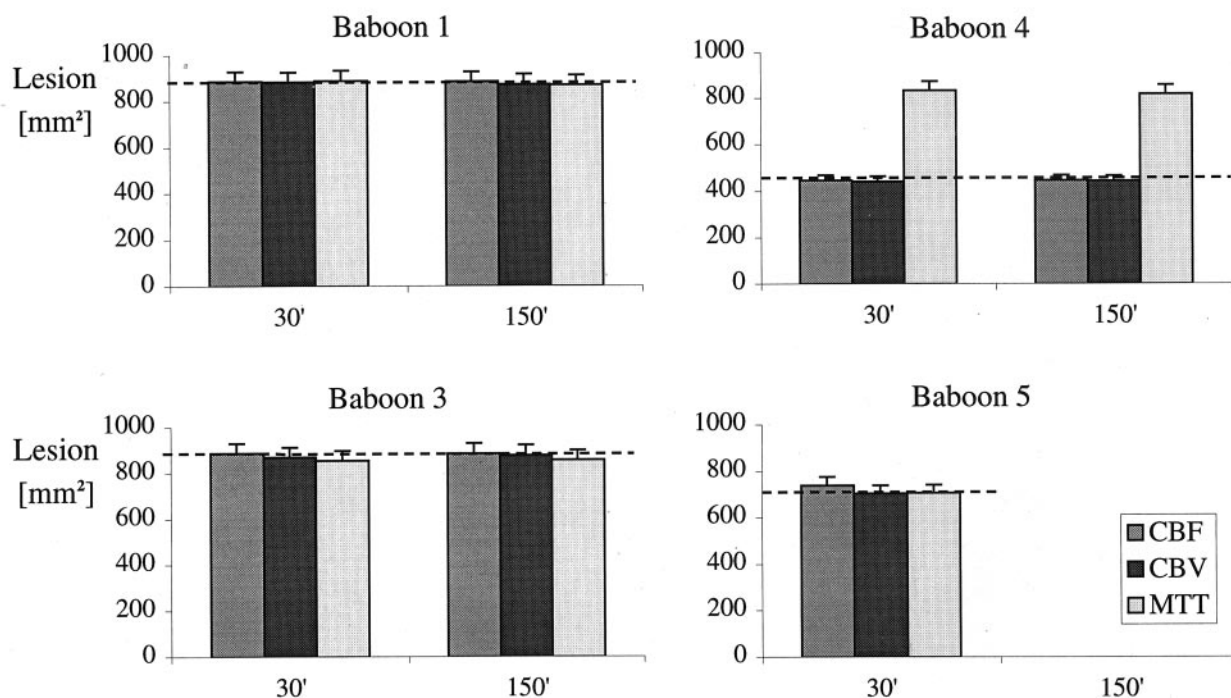
FIG 1. Acutely hypoperfused lesion sizes, as measured with perfusion CT, for animals 1, 3, 4, and 5 at 30- and 150-minute time points after the start of endovascular occlusion. At each time point, the leftmost column corresponds to lesion size (in square millimeters) measured on the CBF map; middle column, lesion size measured on the CBV map; and rightmost column, lesion size measured on the MTT map. The *dashed line* represents outcome infarct size, as determined on the ex vivo T2-weighted MR image. Data for animal 5 were not available at 150 minutes after occlusion because of technical factors.

MCA territory, which manifested itself as a prolonged transit time without an accompanying decrease in CBV or CBF.

The neurobehavioral scores indicated that two of the animals had clinically detectable deficits. Animal 1 had a severe deficit and a score of 4, whereas animal 3 had a moderate deficit and a score of 3. Both severe and moderate scores (scores of 4 and 3) corresponded to the largest infarct sizes of 873 mm^2 ± 10 and 880 mm^2 ± 5. No deficit was observed in two other animals (animals 4 and 5). One animal (animal 3) with clinical deficit had been treated with anti-P-selectin, and the other animal (animal 1) with clinical deficit had not been treated.

In animal 2, the average fCT lesion size decreased during the 3-hour occlusion phase, and at 150 minutes after occlusion, it was only 45% of the size measured at 30 minutes after occlusion (374 vs 837 mm^2). The DSA study, which was performed prior to reperfusion, showed partial deflation of the balloon and some MCA reperfusion, which explained the reduction in the hypoperfused area, as seen on fCT scans. The outcome infarct size was 385 mm^2 ± 6, and no clinical neurologic deficits were observed. A summary of the fCT data for this animal is shown in Figure 6.

Discussion

Clinical studies of neuroprotective and reperfusion strategies in patients with spontaneous cerebral infarction are hampered by uncertain knowledge of the time of occlusion onset, the occurrence of spontaneous reperfusion (if any), and the expected sizes of hypoperfused areas of brain. To address these uncertainties, preclinical studies of techniques for the salvage of brain tissue from infarction require the use of an experimental stroke model that closely mimics the evolution of cerebral ischemia or infarction in humans. The extrapolation of results obtained in nonprimate species may also be unreliable. This difficulty is exemplified by numerous therapeutic stroke trials that have been successful in nonprimate species but then fail in human patients. Thus, preclinical investigations performed by using a model with neuropathologic characteristics similar to those in humans are the most efficient and cost-effective. Such an approach also avoids unnecessary clinical trials, because success in preclinical trials with a primate model is highly likely to apply to clinical practice. Indeed, several experimental studies of stroke physiology and cerebral circulation after controlled vessel occlusion have been performed by using such primate models (1, 6–18). However, all the previously reported models make use of a transorbital approach to achieve MCA occlusion; thus, they are necessarily invasive. In our study, we developed a minimally invasive primate model of stroke by using a neurointerventional endovascular approach to produce MCA vessel occlusion (2). This endovascular model of occlusion and reperfusion is clinically pertinent and can be used for studies of stroke physiology as well as studies of new therapeutic interventions. The minimally invasive na-
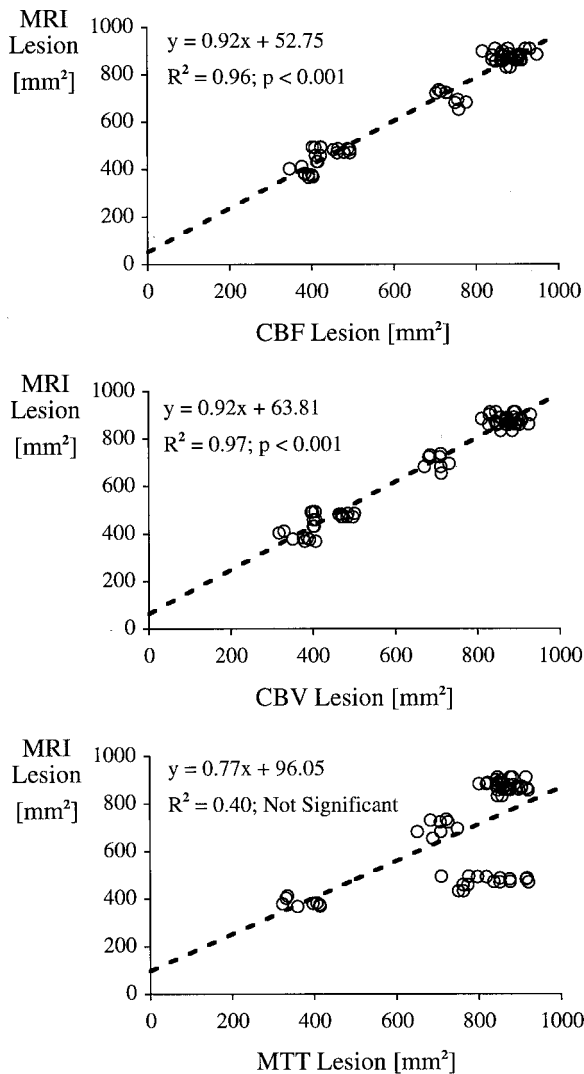
FIG 2. Regression statistics between the CT-determined CBF-, CBV-, and MTT-based lesion sizes and the 48-hour outcome lesion sizes, as measured at ex vivo MR imaging. Each point represents a single measurement by an observer. Scatter represents inter- and intra-observer variations. These variations were not statistically significant, as determined by using ANOVA. Data from animal 2 were not included in this particular analysis because the occluding balloon leaked, with resultant early reperfusion and subsequent reduction in the size of the infarcted region (Fig 6).
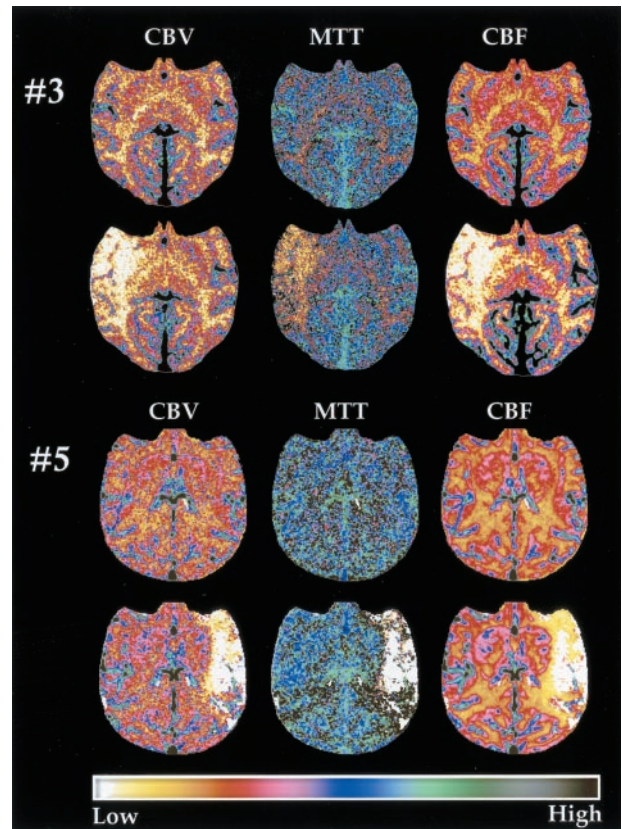

FIG 3. Pre- and postocclusion maps for animals 3 and 5. The *first row* and *third row* from the top present the CBV, MTT, and CBF maps from the control preocclusion study in animals 3 and 5, respectively. The *second row* and *fourth row* from the top present the maps obtained 30 minutes after the onset of MCA occlusion. In animal 3, right MCA territorial hypoperfusion is present, with involvement of the putamen and subtle involvement of the anterolateral thalamus. In animal 5, left MCA territorial hypoperfusion is clearly visible after occlusion, but the basal ganglia are spared. Note that each image is individually windowed to facilitate visualization of the lesions.

ture of the procedure allows survival studies to be performed without disturbing the animal's visual or facial anatomy.

In this study, we found that the size of infarction at 48 hours, as measured by using T2-weighted MR imaging of ex vivo brain, matched the areas of decreased perfusion, as predicted by CBV and CBF mapping at 30 and 150 minutes after occlusion. In two animals, a clinical neurologic deficit was demonstrated: One (animal 1) had a severe clinical deficit (score, 4), and the other (animal 3) had a moderate clinical deficit (score, 3). These same animals had the largest outcome infarcts, namely, 873 mm^2 $\pm$ 10 and 880 mm^2 $\pm$ 5. Two other animals (animals 4 and 5), both without clinical neurologic deficits (score, 0), had

smaller infarct sizes of 475 mm^2 $\pm$ 7 and 704 mm^2 $\pm$ 10. Animal 2, who underwent partial reperfusion between 30 and 150 minutes after occlusion, had no clinical deficit and had the smallest infarct of all, namely, 385 mm^2 $\pm$ 6. A well-controlled model of cerebral ischemia and infarction, such as that used in this investigation, provides accurate time points to determine the onset and duration of vessel occlusion and is essential for the advancement of our understanding of stroke physiology and its evolution. This information has a profound effect on our ability to alter the outcome of ischemic stroke by using different treatment strategies in humans.

In using an animal model as a test bed for the evaluation of neuroprotective agents, chemical thrombolysis, or mechanical reperfusion strategies, knowledge of the size of the infarction being generated is desirable. When imaging is not available during such experimental work, the generation of the infarction must be predictable and reproducible, because no method is available to ascertain how much brain is involved prior to therapeutic intervention. The model described does not require prior knowledge of the
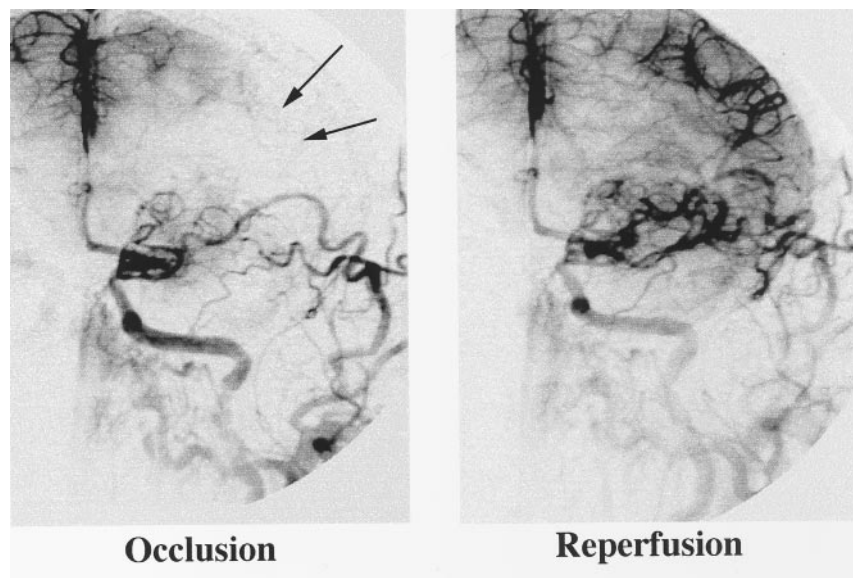
FIG 4. DSA images obtained immediately after MCA occlusion (*left*) and immediately after reperfusion (*right*) in animal 5. During occlusion, the left MCA vessels are absent (*arrows*), but they are clearly seen after reperfusion.
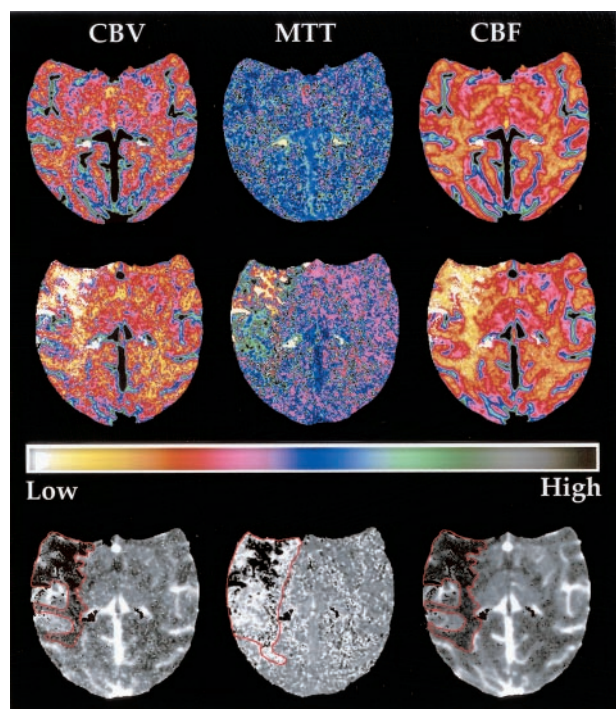

FIG 5. Images in animal 4. *Top row*, CBV, MTT, and CBF maps from the control preocclusion study. *Middle row*, Results from the study obtained 30 minutes after the start of occlusion. The right MCA territorial hypoperfusion is clearly visible after occlusion. *Bottom row*, Examples of ROIs representing the lesion on the maps. The lesion is larger on the MTT map than on the CBV and CBF maps. This is likely due to the presence of collateral circulation that results in normal perfusion on the CBV and CBF maps but prolonged transit time. Each image is individually windowed to facilitate presentation of the lesion.
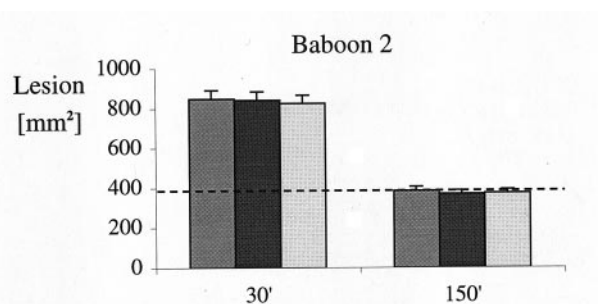

FIG 6. In animal 2, which did not have any neurologic deficit, the balloon leaked between the 30- and 150-minute postocclusion study points. This early reperfusion reduced the outcome size of the lesion. This is an example of a desirable situation in which partial reperfusion of an ischemic territory occurs sufficiently early to substantially reduce the outcome infarct size.

amount of tissue affected by MCA occlusion. CT perfusion imaging performed immediately after the occlusion depicts the actual amount of hypoperfused tissue present. An identical occlusion technique resulted in an infarction size of 700–880 mm^2 in the imaged section, except in animal 4, in which it was 440 mm^2. Examination of the MTT map in this animal, however, reveals a larger lesion (Fig 5). In the event, the final outcome was close to that predicted by using the CBV and CBF maps and not that predicted by using the MTT maps. An explanation for this lies in considering the physiology of collateral flow. Baboon 4 received sufficient blood supply beyond the occlusion to protect approximately half of the territory that would otherwise have become infarcted. The MTT map is sensitive to the length of the path by which perfusing blood reaches a region, and it shows prolonged transit time along collateral vessels that supply blood to the at-risk tissue beyond the occlusion. Animal 2 is an example of unplanned early reperfusion. The initial size of the hypoperfused area is of the same order as that in animals 1, 3, and 5, and we would expect the final infarction to be the same size. However, because of reperfusion due to the leaking balloon, only the tissue that remained without blood supply throughout the 3-hour experiment became infarcted, and this was correctly predicted with the 150-minute imaging study (Fig 6).

Early predictors of the final outcome after stroke onset may assist in better planning of treatment and patient care. We have shown that the final size of

infarction observed at 48 hours after a 3-hour MCA occlusion can be closely predicted as soon as 30 minutes after the onset of occlusion by using CBV or CBF functional maps of cerebral perfusion, as long as no reperfusion interventions are attempted. The CBV and CBF maps both provided robust predictors ($R^2 =$ 0.97 and 0.96, $P < .001$). Bolus-tracking CT perfusion scanning is easily added to the conventional nonenhanced CT protocol and can provide additional predictive information about outcome infarct size. However, bolus tracking CT perfusion scanning is limited to only four sections over 2–3 cm with the current multisection CT scanners. This limitation restricts its value in situations in which an evaluation of the entire brain is required. An alternative for clinical use in patients with signs and symptoms of ischemic stroke undergoing CT immediately after presenting to the emergency room is the use of a whole-brain CT perfusion paradigm that can also be used to identify regional hypoperfusion and predict final infarct size (19).

Tissue survival depends on the duration, as well as on severity, of ischemia (20, 21). In a baboon model of varying lengths of MCA occlusion, Touzani et al (15) showed that, by using CBF imaging with PET, an early restoration of blood flow reverses the progressive derangement of metabolism and markedly limits the final volume of infarction. In our study, we observed this phenomenon in animal 2, who had early and progressive reperfusion of the MCA territory due to balloon leakage. This is an example of a desirable clinical situation in which reperfusion of clearly ischemic territory occurs sufficiently early to result in successful preservation of what would otherwise have become infarcted brain (20).

Because we administered anti-P-selectin to two animals in this study, some characteristics may have changed in these animals. An anti-P-selectin strategy for protection against cerebral lesions induced by arterial occlusion has been proposed in rodents and supported by study findings in knock-out mice treated with an anti-P-selectin antibody (22–24). In addition to the potential desired effect of reducing leukocyte infiltration in the area of the ischemia, anti-P-selectin in both of these studies was shown to work at least partly by improving the regional and relative cerebral blood flow. In our study, we did not observe any effects on cerebral perfusion or the physiologic status of the treated animals versus untreated animals. However, because of the small numbers, no comments can be made regarding possible effects of anti-P-selectin on the basis of these data.

Conclusion

fCT evaluation of vascular physiology, with bolus-tracking first-pass analysis of the movement of contrast agent through the cerebral vasculature, can be used to accurately predict the size of infarction 48 hours after a 3-hour MCA occlusion in a primate model of ischemic stroke. The combination of a minimally invasive approach with high-spatial-resolution measurement of cerebrovascular physiology makes this model highly suitable for use in longitudinal studies of the effects of various therapeutic regimens for ischemic stroke.

Acknowledgment

References

1. Jones TH, Morawetz RB, Crowell RM, et al. **Thresholds of focal cerebral ischemia in awake monkeys.** *J Neurosurg* 1981;54:773–782
2. Morris PP, Maynard K, Lo EH, et al. **Model for stroke in baboons using reversible endovascular occlusion: technical aspects.** In: *ASNR 1995.* Oak Brook, IL: ASNR; 1995
3. Inoue A. **Development of a hybrid CT/angiography system.** *Toshiba Med Rev* 1993;43:9–15
4. Hamberg LM, Hunter GJ, Halpern EF, Hoop B, Gazelle GS, Wolf GL. **Quantitative high-resolution measurement of cerebrovascular physiology with slip-ring CT.** *AJNR Am J Neuroradiol* 1996;17:639–650
5. Hamberg LM, Macfarlane R, Tasdemiroglu E, et al. **Measurement of cerebrovascular changes in cats after transient ischemia using dynamic magnetic resonance imaging.** *Stroke* 1993;24:444–450
6. Branston NM, Symon L, Crockard HA, Pasztor E. **Relationship between the cortical evoked potential and local cortical blood flow following acute middle cerebral artery occlusion in the baboon.** *Exp Neurol* 1974;45:195–208
7. Symon L, Dorsch NW, Crockard HA. **The production and clinical features of a chronic stroke model in experimental primates.** *Stroke* 1975;6:476–481
8. Symon L, Crockard HA, Dorsch NW, Branston NM, Juhasz J. **Local cerebral blood flow and vascular reactivity in a chronic stable stroke in baboons.** *Stroke* 1975;6:482–492
9. Symon L, Branston NM, Strong AJ. **Autoregulation in acute focal ischemia. An experimental study.** *Stroke* 1976;7:547–554
10. Spetzler RF, Selman WR, Weinstein P, et al. **Chronic reversible cerebral ischemia: evaluation of a new baboon model.** *Neurosurgery* 1980;7:257–261
11. Crowell RM, Marcoux FW, DeGirolami U. **Variability and reversibility of focal cerebral ischemia in unanesthetized monkeys.** *Neurology* 1981;31:1295–1302
12. Del Zoppo GJ, Copeland BR, Harker LA, et al. **Experimental acute thrombotic stroke in baboons.** *Stroke* 1986;17:1254–1265
13. Hadley MN, Zabramski JM, Spetzler RF, Rigamonti D, Fifield MS, Johnson PC. **The efficacy of intravenous nimodipine in the treatment of focal cerebral ischemia in a primate model.** *Neurosurgery* 1989;25:63–70
14. Pappata S, Fiorelli M, Rommel T, et al. PET **study of changes in local brain hemodynamics and oxygen metabolism after unilateral middle cerebral artery occlusion in baboons.** *J Cereb Blood Flow Metab* 1993;13:416–424
15. Touzani O, Young AR, Derlon JM, et al. **Sequential studies of severely hypometabolic tissue volumes after permanent middle cerebral artery occlusion: a positron emission tomographic investigation in anesthetized baboons.** *Stroke* 1995;26:2112–2119
16. Young AR, Sette G, Touzani O, et al. **Relationships between high oxygen extraction fraction in the acute stage and final infarction in reversible middle cerebral artery occlusion: an investigation in anesthetized baboons with positron emission tomography.** *J Cereb Blood Flow Metab* 1996;16:1176–1188
17. Young AR, Touzani O, Derlon JM, Sette G, MacKenzie ET, Baron JC. **Early reperfusion in the anesthetized baboon reduces brain damage following middle cerebral artery occlusion: a quantitative analysis of infarction volume [published erratum appears in Stroke 1997 May;28:1092].** *Stroke* 1997;28:632–637
18. Huang J, Mocco J, Choudhri TF, et al. **A modified transorbital baboon model of reperfused stroke.** *Stroke* 2000;31:3054–3063
19. Hunter GJ, Hamberg LM, Ponzo JA, et al. **Assessment of cerebral**

perfusion and arterial anatomy in hyperacute stroke with three-dimensional functional CT: early clinical results. *AJNR Am J Neuroradiol* 1998;19:29–37

20. Bell BA, Symon L, Branston NM. **CBF and time thresholds for the formation of ischemic cerebral edema, and effect of reperfusion in baboons.** *J Neurosurg* 1985;62:31–41

21. Fisher M, Garcia JH. **Evolving stroke and the ischemic penumbra.** *Neurology* 1996;47:884–888

22. Connolly ES, Winfree CJ, Prestigiacomo CJ, et al. **Exacerbation of**

cerebral injury in mice that express the P-selectin gene: identification of P-selectin blockade as a new target for the treatment of stroke. *Circ Res* 1997;81:304–310

23. Suzuki H, Abe K, Tojo SJ, et al. **Reduction of ischemic brain injury by anti-P-selectin monoclonal antibody after permanent middle cerebral artery occlusion in rat.** Neurol Res 1999;21:269–276

24. Suzuki H, Hayashi T, Tojo SJ, et al. **Anti-P-selectin antibody attenuates rat brain ischemic injury.** *Neurosci Letters* 1999;265:163–166